

FILTERING OF CROSS-SPREADS USING MULTICHANNEL SINGULAR SPECTRUM ANALYSIS AND INSTANTANEOUS FREQUENCY METHODS

Misael P. de Souza ¹ and Milton J. Porsani ^{2,3}

ABSTRACT. The orthogonal geometry of 3D seismic data acquisition generates cross-spreads, which are small subsets of multidimensional data. These subsets present unique properties, where ground roll and linear noises become geometrically easy to detect, and multidimensional filters play an essential role in seismic processing. In the present paper, we show the application of combined time-domain Recursive and Iterative Multichannel Singular Spectrum Analysis and average instantaneous frequency methods for random and coherent noise attenuation and enhancement of the reflections in the cross spread. The methodology starts decomposing the cross spread into a set of components, by the recursive-iterative Singular Spectrum Analysis method. The average instantaneous frequency method identifies the low-frequency areas associated with the ground roll to attenuate by muting and stacking each 3D component, where the instantaneous frequency values match the ground roll bandwidth; then the 3D volume filtering is performed by Multichannel Singular Spectrum Analysis, after NMO correction, enhancing the reflections and increasing the lateral coherence in filtered pre-stack seismic data. Numerical experiments using an example of a cross-spread from 3D land seismic data have shown excellent results of the extension of our methodology for random noise and ground roll attenuation in the cross-spread domain.

Keywords: time-series analysis; seismic noise; image processing; Fourier analysis; spatial analysis; cross-spreads; interface waves.

RESUMO. A geometria ortogonal da aquisição de dados sísmicos 3D gera cross-spreads ou lanços cruzados, que são pequenos subconjuntos de dados multidimensional, os quais apresentam propriedades únicas, nos quais ruídos lineares e ground roll tornam-se geometricamente fáceis de serem detectados por filtros multidimensionais. Neste artigo apresentamos uma abordagem de filtragem no domínio do tempo que combina as aplicações do método Análise Espectral Singular e do método de obtenção da frequência média instantânea, que possibilita a atenuação do ground roll e o aumento da coerência lateral das reflexões. A metodologia se inicia com a decomposição dos dados em componentes, através do método Análise Espectral Singular recursiva e iterativa. Essa etapa é seguida da aplicação do método de frequência média instantânea, que permite identificar as áreas de baixa frequência associadas ao ground roll. Assim, efetuamos o silenciamento das amplitudes das componentes, nas áreas em que a frequência média instantânea corresponde à frequência do ground roll. Ao final, fazemos a correção de NMO e aplicamos o método Análise Espectral Singular Recursivo e Iterativo multicanal, que favorece o aumento da coerência lateral das reflexões no dado pré-empilhado. Experimentos numéricos usando um cross-spread de dados sísmicos 3D terrestres mostraram excelentes resultados.

Palavras-chave: geofísica aplicada; processamento digital de sinais; processamento de dados sísmicos; métodos sísmicos.

Corresponding author: Misael Possidonio de Souza

¹ Programa de Pós-Graduação em Geofísica Aplicada (UFBA) (PPGEOF), Instituto de Geociências, Universidade Federal da Bahia, Campus Universitário da Federação, Salvador, Bahia, Brazil – E-mail: misael.geof@gmail.com

² Centro de Pesquisa em Geofísica e Geologia (CPPG/UFBA), Instituto de Geociências, Universidade Federal da Bahia, Campus Universitário da Federação, Salvador, Bahia, Brazil

³ Centro de Pesquisa em Geofísica e Geologia (CPPG/UFBA) and National Institute of Science and Technology of Petroleum Geophysics (INCT-GP/CNPQ)

INTRODUCTION

The seismic acquisition of 3D data has brought several benefits such as complete coverage of offsets with azimuth richness resulting in better images, significant definition of reservoirs and faults, and smaller-scale fracture. Despite the improvements in 3D seismic image quality, various noises such as the ground roll have low-frequency, high amplitude, and coherence. These noises are present in 3D land data and mix with reflections, which is necessary to apply several filtering methods to increase the S/N ratio.

Seismic processing has also brought several benefits, allowing the geometric data organization in particular domains to generate better seismic volumes. Vermeer (2005) defined the 5D data (surface source and receiver coordinates and time) as a collection of subsets known as cross-spreads in the orthogonal geometry of the seismic acquisition. In this unique domain, coherence filters take advantage of the directional correlations and spatial patterns, such as solid linearity in ground roll.

There are methods for seismic filtering well-known by industry in 3D land data seismic processing (Yilmaz, 2001), such as time-variant spectral whitening and the $f - x - y$ deconvolution (Canales, 1984). In the literature, many works have shown the use of rank-reduction methods to filter seismic data. Freire (1986) proposed two-dimensional SVD filtering on seismic data to eliminate this noise; Porsani *et al.* (2009) proposed an adaptive SVD filtering in NMO-corrected source gathers, taking advantage of spatial coherence in flattened; Tyapkin *et al.* (2003) presented a hybrid method combining SVD filtering with a particular linear transformation to remove noise and minimize damage to the signal.

Silva *et al.* (2016) proposed an approach in which the filtering is done by selecting each trace separately from the decomposition of each seismic trace, improving the temporal correlation of the seismic reflections. The classical SSA methodology first creates the original series Hankel matrix and then applies a rank-reduction method in the $f - x$ domain, assuming its signal characteristics and previous structures that one wants to enhance or attenuate (Lari *et al.*, 2019). Porsani *et al.* (2019) presented an approach called RI-SSA in the time-domain, where the selection of high and low-frequency components becomes much more efficient and maintains the signal attributes.

Possidonio and Porsani (2021) presented a technique that combines time-domain multichannel RI-SSA with mean instantaneous frequency (AIF). In this methodology, a CMP is decomposed, and the AIF values for each component are calculated. The associated lower values are linked to the ground roll, muting the region where the values are less than a cut-off frequency and recovering the signal. After that, the processing applies the NMO correction to the data resulting from the previous step and applies the multichannel RI-SSA to improve the lateral coherence, generating valid output

without ground roll and random noise effects.

This work adapts the methodology described in Possidonio and Porsani (2021) to the pre-stack filtering of cross-spread seismic data. We show the application of the time-domain RI-MSSA algorithm as a volume filter in the data. We first selected the ground roll area using the cut-off frequency, and then we applied the 3D operator to the NMO-corrected volume. The results in 3D land data were quite promising, which indicates the substantial importance of this methodology in 3D seismic processing.

ORTHOGONAL GEOMETRY AND CROSS-SPREADS

The intersection of a shot line and a receiving line in a 3D acquisition by an angle of approximately 90 degrees characterizes the orthogonal geometry (Vermeer, 2012). Vermeer (2002), based on these concepts, defines a seismic survey as a 5D data set formed by a sum of smaller 3D subsets, the cross-spreads, with unique characteristics, where its center is formed by each source and receiver line intersection.

The dense spatial distribution of shots and receivers creates a dense coverage of a single area with no obstacles such as houses, roads, and farms, for example, within the survey Vermeer (2002). Figure 1 illustrates the orthogonal geometry of a cross-spread. Within this arrangement, it is possible to combine the lines with a range of offsets and azimuths.

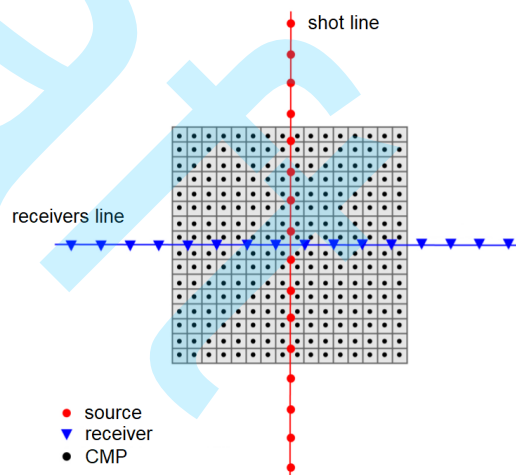


Figure 1. Orthogonal geometry of a cross-spread. The shot line (red) crosses the receiver line (blue) forming this unique domain. Modified from Vermeer (2002).

The same offset lines will have midpoints inside a circle whose diameter is equal to this offset. Thus, in 3D cross-spread, the ground roll will behave as a truly three-dimensional and regular event, having a cone-like shape with its center positioned at the origin. Figure 2 illustrates the time slices of a cross-spread, showing the circular behavior formed by the roller on the ground. These properties facilitate the filtering process in this

domain, such as 3D $f - k$ filtering, geometrical methods, and rank-reduction-based methods exploring the coherence between neighboring seismic traces.

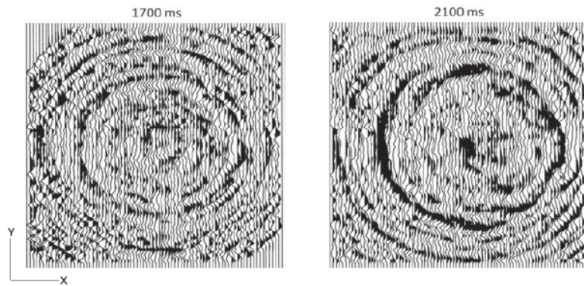


Figure 2. Cross-spread time slices at 1700 ms (left) and at 2100 ms (right). Modified from Vermeer (2002).

Oriented Seismic Processing

Excellent results are well described in the literature (Vermeer, 2005) on the seismic processing of orthogonal geometry data. An example is the attenuation of random and environmental noise, interpolation of shots and receivers, and even first-break peaking estimations for static corrections. These techniques often improve the S/N ratio of the data, leading to more accurate subsurface images.

Inside cross-spread data, the ground roll noise presents 3D behavior, so its spatial coherence may be used by 3D algorithms that improve the S/N ratio of seismic data.

SINGULAR SPECTRUM ANALYSIS

SSA is a methodology for spectral estimation that allows the distinction between strong and weak components and a given signal's high and low-frequency. The classical SSA algorithm is performed at the $f-x$ domain (Cadzow, 1988; Trickett et al., 2010), and contains the following steps (Oropeza and Sacchi, 2011): (i) compute Hankel matrix from an input signal, (ii) perform rank-reduction of Hankel matrix, (iii) obtain the recovered signal via anti-diagonal averaging. Hereabouts, we apply the time-domain SSA algorithm, as introduced in Porsani et al. (2019). We briefly describe the time-domain SSA method and its recursive and iterative time-domain SSA approach (RI-SSA).

Defining a single trace as $\mathbf{d} = [d(0), \dots, d(N)]^T$ with $N+1$ samples, we form a $(K+N+1) \times (K+1)$ Toeplitz matrix, also known as the trajectory matrix (Harris and Yuan, 2010),

$$\mathbf{D}^T = \begin{bmatrix} d(0) & \dots & d(N) & 0 & \dots & 0 \\ 0 & d(0) & \dots & d(N) & \dots & 0 \\ \vdots & \vdots & \ddots & \ddots & \ddots & 0 \\ 0 & 0 & \dots & d(0) & \dots & d(N) \end{bmatrix}, \quad (1)$$

where $k = 0, \dots, K$ represents the number of successive shifts in the vector \mathbf{d} . Singular Value Decomposition (SVD) is a factorization of a real or complex matrix \mathbf{A} of dimensions $m \times n$ in the form $\mathbf{A} = \mathbf{U}\mathbf{\Sigma}\mathbf{V}^T$, where \mathbf{U} is the $m \times m$ unitary matrix of left singular vectors, $\mathbf{\Sigma}$ is the $m \times n$ diagonal matrix of singular values, and \mathbf{V}^T is the $n \times n$ unitary matrix of right singular vectors. The applications of the SVD include computing the pseudoinverse, matrix approximation, and establishment of the rank, range, and null space of a matrix.

The SVD form of \mathbf{D} (Golub and Van Loan, 1996) can be written as,

$$\mathbf{D} = \sum_{k=0}^K \sigma_k u_k v_k^T, \quad (2)$$

where $\{\sigma_k, u_k, v_k\}$ are singular values and singular vectors of the matrix \mathbf{D} .

The convolution between the input signal and the autocorrelation of its right-side singular vector:

$$\tilde{d}_k(n) = \frac{1}{K+1} (d * r_k)(n) \quad (3)$$

where $\{r_k(n)\}$ represents the autocorrelation coefficients of the singular vector v_k . One may find a complete demonstration of equation 3 in (Porsani et al., 2019).

This approach of SSA is performed in the time-domain and considers data as zeros outside the window. In the presented RI-SSA algorithm, the original data are decomposed by using zero-phase filters, which are obtained from the autocorrelation of the eigenvectors (Porsani et al., 2019). The signal components, via the RI-SSA algorithm, are obtained by convolving the original data with zero-phase filters and have the same phase as the original data. However, the non-causal features of the filters produce numerical artifacts outside the data window, that in the numerical examples presented are neither meaningful nor visible. Because the algorithm uses recursion and iterations, it allows for more careful control of the frequency content of the output.

The SSA time-domain decomposition basically requires four steps: (i) compute the autocorrelation coefficients of the input signal, $\{r_d(k)\}, k = 0, \dots, K$ associated to the matrix $\mathbf{D}^T \mathbf{D} = \mathbf{R}$; (ii) compute the eigenvectors $\{v_k\}, k = 0, \dots, K$; (iii) compute the autocorrelation coefficients of the eigenvectors $\{r_k\}, k = 0, \dots, K$; (iv) compute the components, \tilde{d}_k , (Eq. 3).

SINGLE-CHANNEL RECURSIVE AND ITERATIVE SSA (RI-SSA)

Porsani et al. (2019) proposed an efficient time-domain algorithm called RI-SSA, where the signal decomposition is done inside three loops. In the first loop, the high amplitude component is computed by iterating the number of autocorrelation coefficients τ from $(\tau \times \tau)$ Toeplitz covariance matrix \mathbf{R} , by the SVD rank-reduce from \mathbf{R} .

Below we present the RI-SSA algorithm in terms of the eigenvector of the Toeplitz covariance matrix.

Algorithm 1 Recursive and Iterative SSA - (RI-SSA)

Initial vector

$$d_k = \mathbf{d}$$

DO $k = 1, \dots, K$ (Component loop)

$$\hat{\mathbf{d}}_j = d_k$$

DO $j = 1, \dots, J$ (Recursive loop)

$$\tilde{\mathbf{d}}_\tau = \hat{\mathbf{d}}_j$$

DO $\tau = 1, \dots, k$ (Iterative loop)

- Compute the autocorrelation of $\tilde{\mathbf{d}}_\tau$
- Form the matrix \mathbf{R}_τ (of dimension $\tau \times \tau$)
- Compute the first eigenvector v_τ (of dimension $(\tau \times 1)$)

• Compute the autocorrelation of v_τ ,

$$r_\tau = (1, r_\tau(1), \dots, r_\tau(\tau))^T$$

- Update $\tilde{d}_\tau(n) = \frac{1}{\tau+1}(r_\tau * \tilde{d}_\tau)(n)$, (Eq. 3).

END DO

$$\hat{\mathbf{d}}_j = \hat{\mathbf{d}}_j - \tilde{\mathbf{d}}_k$$

END DO

$$\text{Output } x_k = \hat{\mathbf{d}}_j$$

$$d_k = \mathbf{d}_k - \hat{\mathbf{d}}_j$$

END DO

The power method (Golub and Van Loan, 1996) was used to calculate the first eigenvector v_τ , followed by its autocorrelation r_τ , and it is used to obtain the predicted trace \tilde{d}_τ by the Equation 3. We repeated this process by k times, and, in the end, we subtracted the output trace from the input signal, starting the recursive loop.

RECURSIVE AND ITERATIVE MULTICHANNEL SSA (RI-MSSA)

The classical MSSA method allows simultaneous reconstruction and random noise attenuation of seismic records, which consists of organizing the spatial data at a given temporal frequency into a Hankel matrix of blocks that, under ideal conditions, is a matrix of rank k , where k is the number of plane waves in the analysis window (Oropeza and Sacchi, 2011). Additive noise and missing samples will increase the rank of the Hankel matrix of the data block; therefore, by reducing the rank, noise attenuation and recovery of lost features occur. The rank-reduction can be done through SVD.

Possidonio and Porsani (2021) presented a time-domain multichannel RI-SSA (RI-MSSA) to filter the NMO corrected CMP with solid lateral correlation. This simple approach was to reinforce the horizontal coherence between near traces, removing both uncorrelated and correlated noises. Our implementation of time-domain MSSA creates a new trace formed by the samples of neighboring traces inside the window, that allows generating a new trajectory matrix, which has similarities with the single trace case. Therefore, through this approach, we were able to implement a method that is capable of dealing with temporal and spatial cor-

relation and extracting seismic information, attenuating non-coherent noise in these two dimensions.

This RI-MSSA starts intertwining seismic traces into a single seismic trace \mathbf{d} . For three neighboring seismic traces $\mathbf{a} = (a_1, \dots, a_N)^T$, $\mathbf{b} = (b_1, \dots, b_N)^T$, and $\mathbf{c} = (c_1, \dots, c_N)^T$:

$$\mathbf{d} = (a_1, b_1, c_1, \dots, a_N, b_N, c_N)^T. \quad (4)$$

Consequently, the trajectory matrix \mathbf{D} will be represented by the same form of Equation 1, becoming a single channel problem. This algorithm is described below:

Algorithm 2 Recursive-Iterative Multichannel SSA - (RI-MSSA)

1. Form the intertwined trace \mathbf{d} , with L traces,
 2. Run the RI-SSA algorithm 1,
 3. Reorganize back the intertwined output to obtain the filtered traces.
-

AVERAGE INSTANTANEOUS FREQUENCY

Barnes (2007) defines the complex trace as the time function:

$$z = x + jy = ae^{j\theta}, \quad (5)$$

where j represents the imaginary unit, x represents the input seismic trace, y its imaginary part in quadrature, computed by the Hilbert transform of x ; and a represents the amplitude attribute and θ the phase attribute (Taner et al., 1979). The amplitude and phase are given by:

$$a = \sqrt{x^2 + y^2} \quad (6)$$

and,

$$\theta = \arctan \left\{ \frac{y}{x} \right\}. \quad (7)$$

The instantaneous frequency computed by the equation (7) is very susceptible to noise, so we used the equation derived by Porsani et al. (2018),

$$f(t) = \frac{1}{\pi\Delta t} \text{Im}\{\log(1 + c(t))\}, \quad (8)$$

where $c(t)$ is the reflection coefficient, calculated by Burg's algorithm (Burg, 1975). We computed the AIF values along the seismic trace by using a time sliding window of $2L + 1$ data samples, centered at position n , with time sample interval Δt , $\{z(n - L\Delta t), \dots, z(n), \dots, z(n + L\Delta t)\}$.

PROPOSED METHODOLOGY FOR CROSS-SPREAD GROUND ROLL FILTERING

Taking advantage of the unique properties of cross-spread geometry, the ground roll and other coherent noises present a linear behavior. Besides, this kind

of noise exhibits low-frequency, high amplitude, and a right cone inside a cross-spread. Its lateral coherence is small compared to the seismic reflections, so the ground roll attenuation becomes more robust to explore these combined properties.

For a given cross-spread, the main steps are described as follows:

1. Select the ground roll area inside the cross-spread,
2. Apply the RI-SSA algorithm to decompose the data,
3. Compute the AIF for each component,
4. Mute the data inside the ground roll area, (step [i]) using a cut-off frequency value for AIF,
5. Apply NMO correction and RI-MSSA to generate the filtered output.

Following [Possidonio and Porsani \(2021\)](#), we use the low-frequency and ground roll geometric features to mute the components based on their AIF computed values for a given cross-spread. In this stage, we may apply an amplitude gain to increase the signal content.

After that, the filtered cross-spread presented a considerable attenuation, having the input to the second stage. The main idea was to increase the lateral coherence of neighbor traces inside a small volume of data.

We performed the RI-MSSA filtering by collecting the traces from inlines and cross-lines inside a 3D operator. The RI-MSSA filtering removed random and coherent noises, which did not have lateral coherence than seismic reflections. After filtering, we used NMO inverse correction, generating the filtered output.

APPLICATIONS

This section shows RI-SSA and RI-MSSA methods to filter random noise and ground roll in a cross-spread selected from the 3D data. One can prove the effectiveness of these methods for reducing the amplitudes of coherent noises and maintaining signal amplitudes, increasing the coherence of reflections.

Example of Cross spread

The method presented here assumes a spatial coherence inside the data, that can be achieved by the application of a NMO correction, for example. We strongly recommend the filtering processing application after the preprocessing flow, such as geometry, static correction, and amplitude manipulation. Since the application is done in the time-domain, a poor preprocessing flow negatively affects the filtering process and also other steps. Static corrections must be applied before and it is mandatory in all land data seismic processing. Poor static correction not only misleads us to wrong results in seismic processing but also leads us to wrong interpretation of seismic reflections and subsurface, structures, and velocities. [Possidonio and Porsani \(2021\)](#) showed

Table 1. Seismic acquisition parameters of the selected cross-spread.

Source interval	20 m
Receiver interval	20 m
Shot Line	1
Receiver Line	1
Record length	2000 ms
Number of shots	40
Number of channels	40
Number of samples	1001

that amplitude equalization of seismic data before the application of RI-MSSA generates better results, but it is not a requirement for the method. However, for the seismic processing flow, it is mandatory the recovery of lost amplitude due to the spherical divergence, especially in 3D land data. Therefore, the preprocessing step is quite important before the application of any filtering processing.

Algorithm 2 can be modified to perform spatial filtering in cross spreads after an NMO correction. As we described before, a previous or initial velocity field for NMO correction is known.

In this work, we selected a cross-spread from the seismic survey acquired in the Blackfoot field near Strathmore, Alberta (Township 23, Range 23 W4), [Lawton et al. \(1995\)](#) numerical experiment (Fig. 3). Table 1 shows the seismic acquisition parameters of the selected cross-spread. The 3D visualization is available, as one can see the original in Figure 3. We computed the AIF of this data and illustrated this AIF volume in Figure 4, where the low-frequency attribute value indicates the ground roll zone.

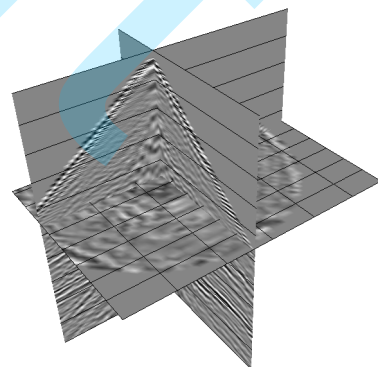


Figure 3. Original volume selected for our study.

The region corresponding to the cone in Figure 4 has low instantaneous frequency values, corresponding to the ground roll part. Inside this part, the ground roll strongly masks the seismic reflections, making it impossible to see. We can observe additional linear noises that also mix with the seismic reflections. We calculated

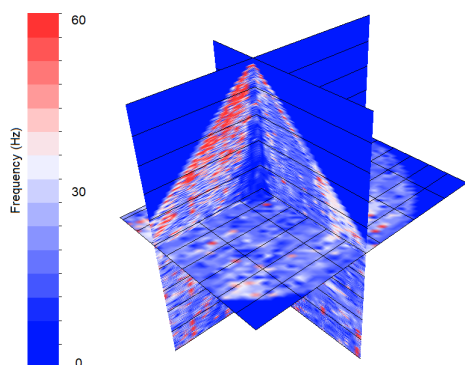


Figure 4. Three-dimensional visualization of computed AIF from data of Figure 3.

and applied an initial amplitude gain for this selected cross-spread to equalize the signal amplitude, aiming for better results.

We started with the original RI-SSA decomposition (algorithm 1), followed by muting the amplitudes where the AIF values were lower than 4 Hz. Figure 5 shows the results from this step. One can see the central inline of the cross-spread in Figure 5a. This RI-SSA decomposition was performed with $J = 10$ recursions, $N = 20$ iterations and $K = 7$ components. After applying the RI-SSA decomposition and zeroing the amplitudes in the areas of occurrence of the ground roll in each component, one can stack the results to estimate the ground roll. Figures 5b and 5c show the decomposed output and the residue from this process, where we applied the AIF-guided mute to the seismogram's internal region, which predominated the ground roll.

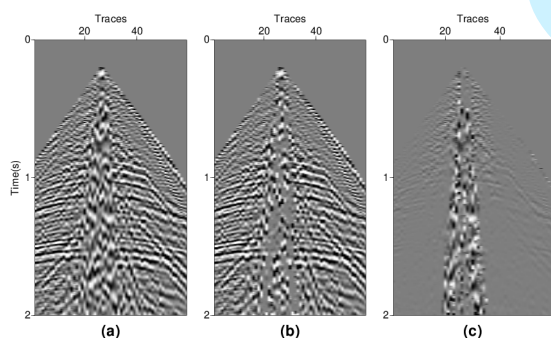


Figure 5. Original central inline in (a); its output from RI-SSA and AIF decomposition (b); and the difference in (c).

Figure 6 illustrates the amplitude spectra of the original cross-spread (black), which was computed using all traces, the ground roll estimation (blue), and the filtered output (red).

We performed the RI-MSSA procedure with the cross-spread from the previous step, where Figure 7a shows the central inline. After organizing the data to the CMP geometry, we applied the NMO correction, where we used the following parameters for the RI-MSSA filtering: a cubic operator with five traces inline and cross-

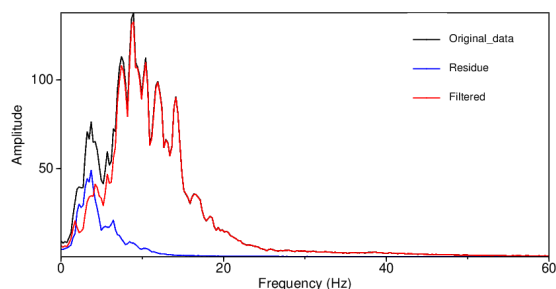


Figure 6. Amplitude spectra of Figure 5a, black line; Figure 5b, red line; and Figure 5c, blue line.

line direction, $J = 21$ iterations, and $N = 31$ recursions. We chose the number of iterations and recursions after analyzing the best results for each data set. This form can select how much information is to be chosen in the inline and crossline directions, filling the trajectory matrix. Once again, Figure 7c shows the central inline of this filtered cross-spread and its corresponding residue in Figure 7b.

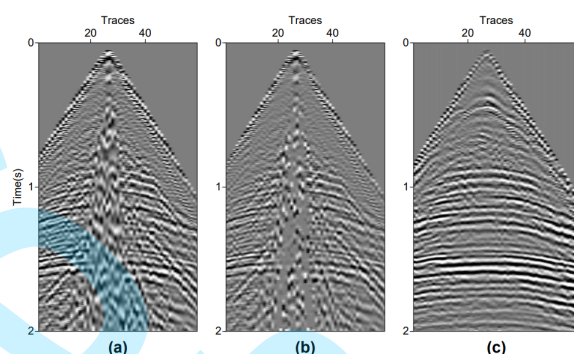


Figure 7. Figure 7c shows the central inline of this filtered cross-spread and its corresponding RI-SSA and AIF decomposition result in Figure 7b. Original inline in Figure 5a.

Figure 8 shows the average amplitude spectra of the original data (black), the decomposed (blue), and RI-MSSA output (red). One could see how each process affects the original spectra and control it by changing the number of iterations, recursions, and components of the filtering process.

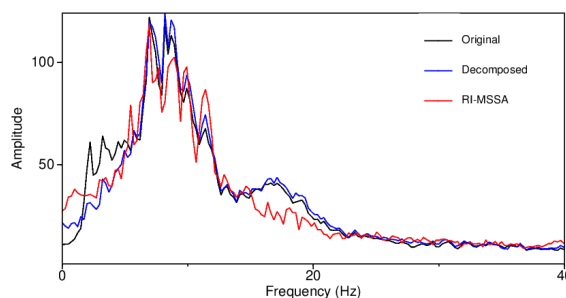


Figure 8. Amplitude spectra of Figure 7a, black line; Figure 7b, blue line; and Figure 7c in (c), red line.

Figure 9 shows the central crossline from the original data in Figure 9a, decomposed data in Figure 9b, and filtered data in Figure 9c. One can note that the reflections overlapped by the coherent noise become visible after the RI-MSSA filtering and the remarkable improvement in the S/N ratio. We notice seismic reflections around 1.0 s to 2.0 s overlapped by the irregular noise patterns. One could see how the filtering reconstructs the lost reflections inside the ground roll area. It is possible to note the reflections between 1.0 s and 2.0 s in the central area after filtering. The cross-spread geometry provides new forms of exploring data information.

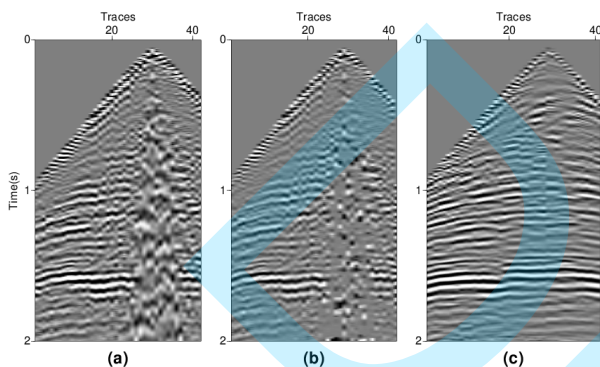


Figure 9. Original cross-line from cross spreading (a), results from RI-SSA and AIF decomposition in (b) and the filtered output cross-line in (c).

One could see the highly masked reflections by ground roll before the filtering in Figures 10a and 10b.

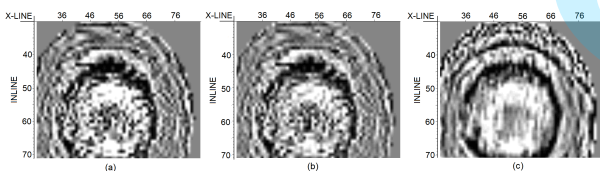


Figure 10. Time-slices at 1000 ms from original cross-spread in (a); its RI-SSA and AIF decomposition in (b); and the filtered RI-MSSA output in (c).

Figure 11 shows the results of the application of the RI-MSSA algorithm in the cross-spread domain. Note that in addition to the ground roll filtering, the filter reinforces the spatial coherence in the data volume at each time slice, filtering the present random noises.

Finally, we can visualize the positive results and regions of high coherence more visible in the 3D output data. Before filtering, it is undeniable the low quality and S/N ratio. At the same time, the output presents a higher S/N ratio, high-quality reflections with significant amplitudes and frequency, which can be remarkably useful for other steps such as seismic migration and velocity analysis.

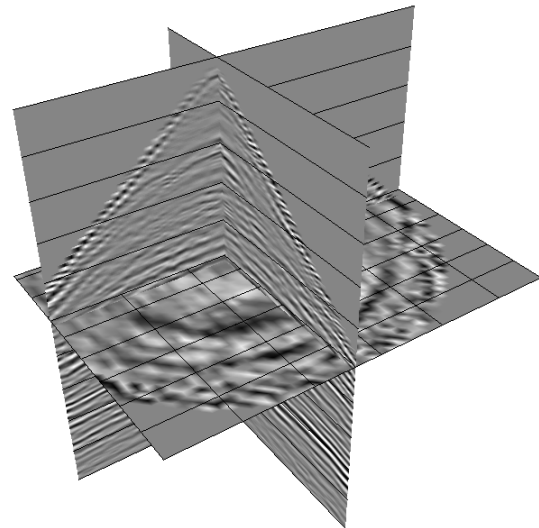


Figure 11. Filtered output of the cross-spread in Figure 4 after application of our methodology.

CONCLUSION

We studied the application of our methodology to pre-stack 3D data in the cross-spread domain. The time-domain RI-SSA was first used to better decompose the signal; the AIF input data computation provided better ground roll selection based on the small frequency values that matched those frequencies inside the ground roll geometrical cone. The multi-channel RI-SSA was then applied to NMO-corrected rearranged to improve the lateral coherence of seismic reflection data. This technique was slightly modified to become a 3D operator. We showed that numerical results of the processing to one cross-spread could lead to great pre-stack seismic data filtering results, so we strongly suggest the proposed methodology for ground roll filtering in the cross-spread domain, as it takes advantage of this unique domain to remove coherent noise. The results also showed that random noise could be easily removed as they present zero horizontal coherence in seismic data.

ACKNOWLEDGMENTS

We would like to thank to INCT-GP/CNPq/MCT, ANP, Petrobras, FINEP, and FAPESB Brazil for financial support. MPdS thanks the Coordenação de Aperfeiçoamento de Pessoal de Nível Superior (CAPES) for the fellowship in the course of his PhD program.

DATA AVAILABILITY

The 3D-3C Blackfoot data set that supports the findings of this study was created and maintained by CREWES project (<https://www.crewes.org/>).

REFERENCES

- Barnes, A.E. A Tutorial on Complex Seismic Trace Analysis. *GEOPHYSICS* **2007**, *72*, W33–W43. [10.1190/1.2785048](https://doi.org/10.1190/1.2785048).
- Cadzow, J. Signal Enhancement—a Composite Property Mapping Algorithm. *IEEE Transactions on Acoustics, Speech, and Signal Processing* **1988**, *36*, 49–62. [10.1109/29.1488](https://doi.org/10.1109/29.1488).
- Canales, L.L. Random Noise Reduction. In *SEG Technical Program Expanded Abstracts 1984*; SEG Technical Program Expanded Abstracts, Society of Exploration Geophysicists, 1984; pp. 525–527. [10.1190/1.1894168](https://doi.org/10.1190/1.1894168).
- Freire, S.L.M. Aplicações Do Método de Decomposição Em Valores Singulares No Processamento de Dados Sísmicos. PhD thesis, Universidade Federal da Bahia, 1986.
- Golub, G.H.; Van Loan, C.F. *Matrix Computations*, third ed.; The Johns Hopkins University Press, 1996.
- Harris, T.J.; Yuan, H. Filtering and Frequency Interpretations of Singular Spectrum Analysis. *Physica D: Nonlinear Phenomena* **2010**, *239*, 1958–1967. [10.1016/j.physd.2010.07.005](https://doi.org/10.1016/j.physd.2010.07.005).
- Lari, H.H.; Naghizadeh, M.; Sacchi, M.D.; Gholami, A. Adaptive Singular Spectrum Analysis for Seismic Denoising and Interpolation. *GEOPHYSICS* **2019**, *84*, V133–V142. [10.1190/geo2018-0350.1](https://doi.org/10.1190/geo2018-0350.1).
- Lawton, D.C.; Stewart, R.R.; Cordsen, A.; Hrycak, S. Advances in 3C-3D Design for Converted Waves. Technical report, CREWES Project, 1995.
- Oropeza, V.; Sacchi, M. Simultaneous Seismic Data Denoising and Reconstruction via Multichannel Singular Spectrum Analysis. *GEOPHYSICS* **2011**, *76*, V25–V32. [10.1190/1.3552706](https://doi.org/10.1190/1.3552706).
- Porsani, M.J.; Silva, M.G.; Melo, P.E.M.; Ursin, B. Ground-Roll Attenuation Based on SVD Filtering. In *SEG Technical Program Expanded Abstracts 2009*; SEG Technical Program Expanded Abstracts, Society of Exploration Geophysicists, 2009; pp. 3381–3385. [10.1190/1.3255563](https://doi.org/10.1190/1.3255563).
- Porsani, M.J.; Ursin, B.; G. Silva, M. Signal Analysis and Time-Frequency Representation Using SSA and Adaptive AR Methods. In *SEG Technical Program Expanded Abstracts 2018*; SEG Technical Program Expanded Abstracts, Society of Exploration Geophysicists, 2018; pp. 5022–5026. [10.1190/segam2018-2995661.1](https://doi.org/10.1190/segam2018-2995661.1).
- Porsani, M.J.; Ursin, B.; Silva, M.G. Signal Decomposition and Time-Frequency Representation Using Iterative Singular Spectrum Analysis. *Geophysical Journal International* **2019**, *217*, 748–765. [10.1093/gji/ggz046](https://doi.org/10.1093/gji/ggz046).
- Possidonio, M.; Porsani, M.J. A Combined Method Using Singular Spectrum Analysis and Instantaneous Frequency for the Ground-Roll Filtering. *Geophysical Journal International* **2021**, *226*, 446–455. [10.1093/gji/ggab082](https://doi.org/10.1093/gji/ggab082).
- Silva, M.; Porsani, M.; Ursin, B. A Single-Trace Singular-Value Decomposition Method with Application to the Ground-Roll Removal. In *SEG Technical Program Expanded Abstracts 2016*; SEG Technical Program Expanded Abstracts, Society of Exploration Geophysicists, 2016; pp. 4659–4663. [10.1190/segam2016-13866459.1](https://doi.org/10.1190/segam2016-13866459.1).
- Taner, M.T.; Koehler, F.; Sheriff, R.E. Complex Seismic Trace Analysis. *GEOPHYSICS* **1979**, *44*, 1041–1063. [10.1190/1.1440994](https://doi.org/10.1190/1.1440994).
- Trickett, S.; Burroughs, L.; Milton, A.; Walton, L.; Dack, R. Rank-Reduction-Based Trace Interpolation. In *SEG Technical Program Expanded Abstracts 2010*; SEG Technical Program Expanded Abstracts, Society of Exploration Geophysicists, 2010; pp. 3829–3833. [10.1190/1.3513645](https://doi.org/10.1190/1.3513645).
- Tyapkin, Y.K.; Marmalyevskyy, N.Y.; Gorniyak, Z.V. Source-Generated Noise Attenuation Using the Singular Value Decomposition. In *SEG Technical Program Expanded Abstracts 2003*; SEG Technical Program Expanded Abstracts, Society of Exploration Geophysicists, 2003; pp. 2044–2047. [10.1190/1.1817733](https://doi.org/10.1190/1.1817733).
- Vermeer, G.J.O. *3-D Seismic Survey Design*; Geophysical References Series, Society of Exploration Geophysicists, 2002. [10.1190/1.9781560801757](https://doi.org/10.1190/1.9781560801757).
- Vermeer, G.J.O. Processing Orthogonal Geometry - What Is Missing? In *SEG Technical Program Expanded Abstracts 2005*; SEG Technical Program Expanded Abstracts, Society of Exploration Geophysicists, 2005; pp. 2201–2204. [10.1190/1.2148152](https://doi.org/10.1190/1.2148152).
- Vermeer, G.J.O. *3D Seismic Survey Design*; SEG Books, 2012.
- Yilmaz, Ö. *Seismic Data Analysis*; Investigations in Geophysics, Society of Exploration Geophysicists, 2001. [10.1190/1.9781560801580](https://doi.org/10.1190/1.9781560801580).

M.P.S.: computational implementation of the RI-MSSA algorithm, data pre-processing, figure generation, writing of the article; **M.J.P.:** monitoring and supervision of the results obtained, writing of the article.

Received on December 16, 2021/ Accepted on March 25, 2022.



-Creative Commons attribution-type BY